IEEE Access
Multidisciplinary ⋮ Rapid Review ⋮ Open Access Journal

Received 10 April 2024, accepted 18 April 2024, date of publication 26 April 2024, date of current version 10 May 2024.

Digital Object Identifier 10.1109/ACCESS.2024.3393943

RESEARCH ARTICLE

A Rotary Wireless Power Transfer System With Rail-Type Coupling Structure

KUN XIA, BENJING ZHU, YANG LOU, AND DAMING HUANG
Department of Electrical Engineering, University of Shanghai for Science and Technology, Yangpu, Shanghai 200093, China

Corresponding author: Benjing Zhu (212221688@st.usst.edu.cn)

This work was supported in part by the National Local Joint Engineering Laboratory of High Energy Saving Motor and Control Technology Open Subject under Grant KFKT202105.

ABSTRACT Traditional power supply methods for rotating mechanisms are found to face problems, including complex structures, limited functionality, and potential safety hazards. To address these problems, a rotary wireless power transfer system with new rail-type coupling structure (RTR-WPT) is proposed in this paper. This system, characterized by safety, reliability, and flexible installation, is designed to provide power to devices mounted on rotating shafts. Firstly, the topological structure of the RTR-WPT system is introduced, and the corresponding circuit model is established. Secondly, MAXWELL is utilized for finite element analysis to design and optimize the rail-type rotary coupler. Finally, an experimental platform for the RTR-WPT system is built and tested. From the experimental results, it is validated that the new rail-type coupler and the design methodology are feasible, and the system can achieve a power transmission of 10.33W with an overall efficiency of 72.1% under rotating conditions.

INDEX TERMS Rotating mechanism, rail-type coupling structure, wireless power transfer, finite element analysis.

I. INTRODUCTION

This Currently, rotary electrical equipment is widely used in the industrial field. The primary methods for powering rotating components include conductive slip ring power supply, battery power supply, and rotary transformer power supply, among others [1], [2], [3]. The sliding contact method between brush and collector ring is adopted by the slip ring power supply. Although its technology is relatively mature and widely used, it still faces problems such as sliding wear, localized overheating, and contact sparking, resulting in poor reliability [4], [5], [6]. Battery power supply is simple in principle, but it is constrained by its finite electrical energy and safety concerns. The application of rotary transformers has greatly improved the overall reliability and service life of equipment. However, their low-frequency characteristics necessitate a small working air gap, typically only 1 millimeter or less, limiting their application in situations involving large vibrations and impacts [7], [8].

The associate editor coordinating the review of this manuscript and approving it for publication was Ton Duc Do.

Wireless power transfer (WPT) technology, which enables non-contact electrical energy transmission through resonant coupling coils, overcomes many shortcomings of traditional contact-based power supply methods. It has the advantages of flexibility, safety, reliability, and strong environmental adaptability [9], [10], [11]. In recent years, WPT has played a significant role in various fields such as robotics, drones, electric vehicles, and medical equipment [12], [13], [14], [15], [16]. It also provides a new direction for the power supply of rotating electrical equipment and attracts more and more attention. In order to accommodate different scenarios, various types of rotary wireless power transfer(R-WPT) schemes have been proposed by researchers [17], [18], [19], [20]. Reference [17] proposed a R-WPT system for solar wing driving of the spacecraft. It is characterized by high efficiency, wear-free, safe, and reliable operation. However, the development of this system is limited by its large size and low integration. Reference [18] introduced an inductive wireless power transfer system for real-time monitoring of the ship rotating shafts. The coupling structure is implemented by using multiple decentralized transmitting and receiving

coils, achieving a power capacity of 1.75 W and an efficiency of 75%. However, the stability, integration, and transmission power of this system need to be improved. Reference [19] proposed a R-WPT system based on a mixed flux coupler and dual-path parallel compensation. The two outputs are connected to the axial coupler and the radial coupler respectively. The system can achieve accurate speed monitoring and stable wireless power transmission. However, the installation of this full-ring coil structure is not convenient. Reference [20] presented a R-WPT system based on U-shaped core coupling mechanism with a primary coil. The system can obtain 1.72 w output power with 51.19% transfer efficiency. In summary, the current R-WPT schemes face problems such as inconvenient installation structures, vulnerability to positional offsets, and limited application scenarios. The research on the analysis and design of R-WPT systems still needs to be further improved.

Considering the challenges faced in current research, this paper proposes a rotary wireless power transfer system with a novel rail-type coupling structure (RTR-WPT). The rail-type coupling structure enables quick and convenient installation and disassembly. It effectively reduces component interference, thereby ensuring stability and reliability in power transmission for rotating equipment. Additionally, the compact size of this structure allows for its utilization even in confined spaces. The remainder of this paper is structured as follows. In Section II, the overall structure and working principles of the RTR-WPT system are analyzed. In Section III, the system topology is introduced and the equivalent circuit model based on the S-S compensation network is presented. In Section IV, a rail-type rotary coupling structure is proposed, along with the provision of the corresponding parameters design methodology. In Section V, an experimental prototype of the RTR-WPT system is constructed and tested, verifying its feasibility. In Section VI, the conclusion is presented and the future direction for experimentation is proposed.

II. SYSTEM STRUCTURE AND PRINCIPLE

The proposed RTR-WPT system belongs to the magnetic coupling resonance wireless power transfer system. There are primarily three components, the transmitting side circuit, the energy transfer circuit, and the receiving-side circuit. The core component is the rail-type rotary coupler which is composed of transmitting coils, receiving coils, shell, and ferrite. The 3-D schematic diagram of RTR-WPT is shown in Fig. 1. The DC power supply, high-frequency inverter, and primary compensation circuit are connected to the transmitting coils. The secondary compensation circuit and rectifier are connected to the receiving coils on the rotating shaft.

The operating principle is as follows. A resonant cavity is formed by inductors and capacitors. When the DC power supply is converted into AC excitation at the resonant cavity's natural frequency through the inverter circuit and applied to the transmitting coils, the resonant cavity occurs strong magnetic coupling resonance. Energy can be transferred most

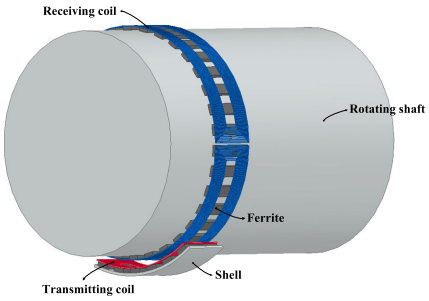

FIGURE 1. 3-D schematic diagram of RTR-WPT.

efficiently and effectively between different circuits. After the magnetic field energy is coupled to the receiving coils, it generates alternating current, which is then converted into direct current through rectifier circuit to enable power supply to the equipment on the rotating shaft.

III. SYSTEM TOPOLOGY AND CIRCUIT MODEL

The system topological structure is shown in Fig. 2, mainly including half-bridge inverter circuit, S-S compensation network, coupler, and rectifier circuit. The system in this paper is classified as low-power with a high operating frequency. Therefore, the inverter circuit employs a half-bridge configuration. This configuration offers advantages such as low switching losses at high frequencies, simple driving circuit, and strong resistance to bias magnetism. WPT system has four basic compensation methods, series-series (S-S), series-parallel (S-P), parallel-series (P-S), and parallel-parallel (P-P). The P-S and P-P compensation topologies are less commonly used due to their complexity, lower output power, and greater fluctuations. The S-P compensation topology is more suitable for systems under heavy-load conditions. The S-S compensation topology features a simple structure and ease of achieving load independence, and the output power and transmission efficiency of the system are easy to control. Additionally, it is more suitable for practical applications [21], [22], [23], [24]. Thus, this paper opts for the S-S compensation network. I_{DC} and U_{DC} are the input current and the voltage of the DC power supply, respectively, I_{out} and U_{out} are the output current and voltage, respectively, L_T and L_R represent the self-inductance of the transmitting

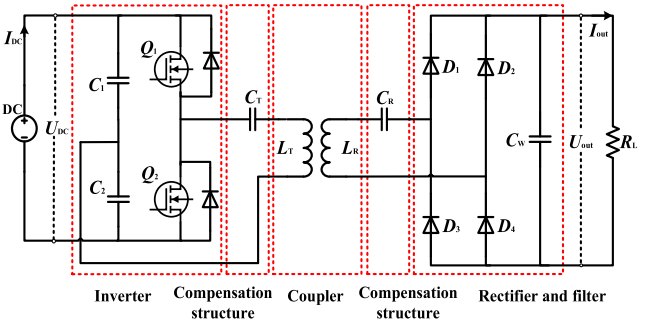

FIGURE 2. RTR-WPT system topology.

and receiving coils, respectively. C_T and C_R represent the compensation capacitance on the transmitting and receiving sides, respectively. The rectifier circuit employs a commonly used bridge configuration. C_W is the output filtering capacitor, and R_L is the load.

The equivalent circuit model of the WPT system based on the S-S compensation topology is shown in Fig. 3, where R_1 and R_2 are the parasitic resistances of the primary circuit and secondary circuit, respectively, R_e is the equivalent AC load, M is the mutual inductance between the transmitting coils and receiving coils. $\dot{U}_P$ is the phasor of the primary input voltage, $\dot{U}_S$ is the secondary output voltage. $\dot{I}_P$ and $\dot{I}_S$ are the primary current phasor and secondary current phasor, respectively.

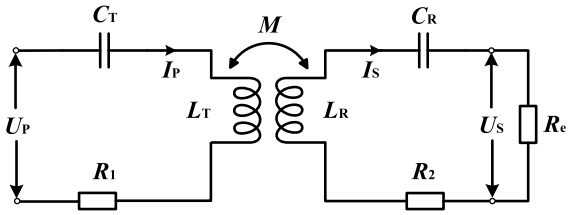

FIGURE 3. Equivalent circuit model based on the S-S compensation topology.

For both the primary circuit and the secondary circuit, according to Kirchhoff's voltage law, the following equation can be obtained:

$$\begin{cases} \left(R_1 + j\omega L_T + \dfrac{1}{\mathrm{j}\omega C_T}\right)\dot{I}_P - \mathrm{j}\omega M\dot{I}_S = \dot{U}_P \\ \left(R_2 + R_e + j\omega L_R + \dfrac{1}{\mathrm{j}\omega C_R}\right)\dot{I}_S - \mathrm{j}\omega M\dot{I}_P = 0 \end{cases} \tag{1}$$

When $jwL_T+1/jwC_T = 0$, $jwL_R+1/jwC_R = 0$, the following equation can be obtained:

$$\begin{cases} \dot{I}_P = \dfrac{\dot{U}_P(R_2 + R_e)}{R_1(R_2 + R_e) + \omega^2 M^2} \\ \dot{I}_S = \dfrac{j\omega M\dot{U}_P}{R_1(R_2 + R_e) + \omega^2 M^2} \\ \dot{U}_S = \dfrac{j\omega M\dot{U}_P R_e}{R_1(R_2 + R_e) + \omega^2 M^2} \end{cases} \tag{2}$$

The transmission efficiency η and transmission power P_{out} of the RTR-WPT system based on the S-S compensation topology can be obtained as follows:

$$\begin{cases} P_{out} = \dfrac{\omega^2 M^2 R_e U_P^2}{\left(R_1 (R_2 + R_e) + \omega^2 M^2\right)^2} \\ \eta = \dfrac{P_{out}}{\dot{U}_P\dot{I}_P} = \dfrac{\omega^2 M^2 R_e}{R_1 (R_2 + R_e)^2 + (R_2 + R_e)\omega^2 M^2} \end{cases} \tag{3}$$

From the above formulas, it can be seen that for the WPT system with S-S compensation network, the values of P_{out} and η are related to the mutual inductance coefficient M, equivalent AC load R_e, and resonant frequency f. Since mutual inductance is correlated with the number of coil turns, the distance between transmitting coils and receiving coils, further analysis can reveal that the values of P_{out} and η are also related to the turns and distance. Furthermore, the rotational speed does not directly affect the output of the rotating wireless power supply system, as crucial parameters such as induced electromotive force and mutual inductance do not rely on the rotational speed. These parameters primarily depend on the shape, size, relative position of the coils, and the rate of change of the current, rather than the rotational speed. In practical applications, high rotational speeds may result in increased mechanical stress and vibration, indirectly impacting the stability and efficiency of the system.

IV. DESIGN OF RAIL-TYPE ROTARY COUPLER

The rail-type rotary coupler proposed in this paper is composed of two planar square coils, the transmitting coils fixed on one side and the receiving coils wrapped around the outer surface of an axis, installed coaxially. The magnetic flux direction distributes along the rotor radius, and the schematic diagram of rail-type rotary coupler is shown in Fig. 4. The use of the rail-type coupling coils winding method can improve the reliability of the system in a rotating state and facilitate installation and disassembly. Taking into consideration the frequency ranges applicable to the Qi and PMA standards, as well as the hardware platform used, this paper selects 100kHz as the resonance frequencies.

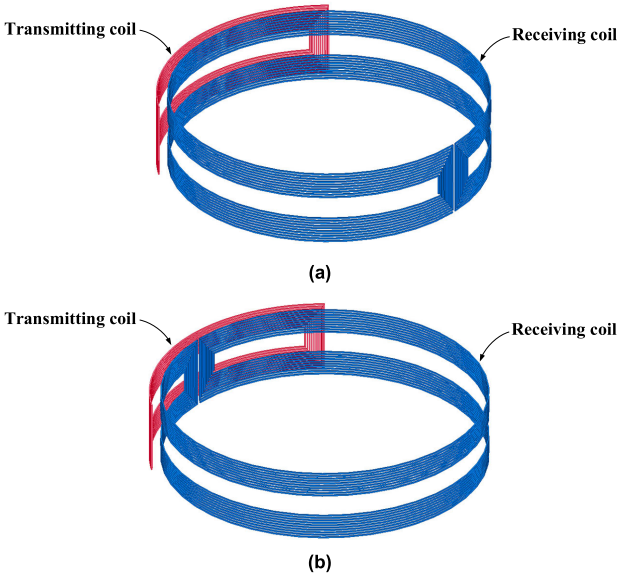

FIGURE 4. Schematic diagram of rail-type coupler. (a) 0°. (b) 180°.

The coils of the system coupler adopt planar coils due to their small size and better coupling effect. Commonly used planar coils are generally divided into circular and square types. With the aid of Maxwell software, a simulation analysis on both planar circular and square coils with the same maximum outer diameter and number of coil turns is conducted in this paper. The resulting magnetic field distribution of these two types of coils are shown in Fig. 5. Through comparison, it can be observed that the magnetic field inside the

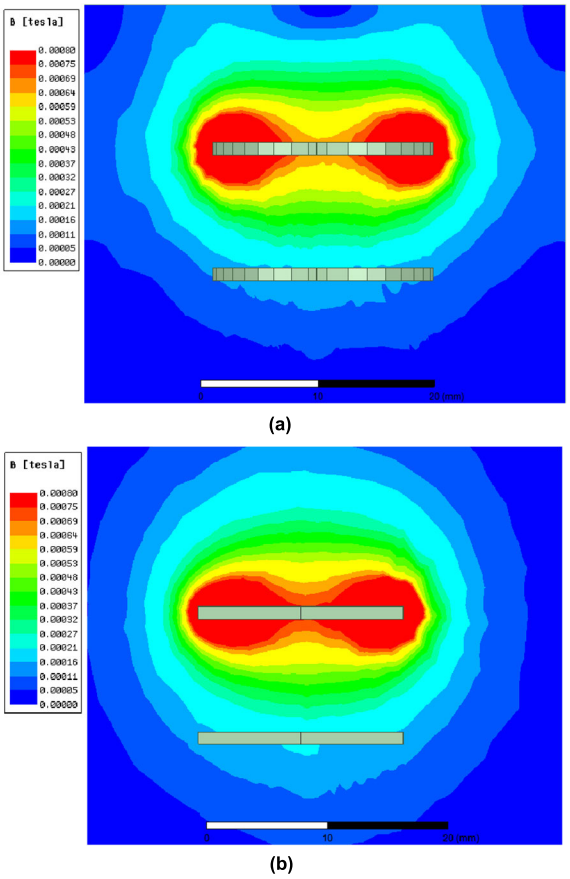

FIGURE 5. Magnetic field distribution diagram of different planar coils. (a) Circular coils. (b) Square coils.

planar square coils is stronger, resulting in a larger effective area for energy transmission.

The test on the resistance to static offset of circular and square coils was conducted. The coupling coefficient variation curves of the two models when they deviate from the center of the circle by a certain distance are shown in Fig. 6. It can be seen that the coupling coefficient of the square coils is larger and the variation is slightly smoother. Taking into account the fitting method at both ends of the coils, the winding method of the square coils is chosen in this paper.

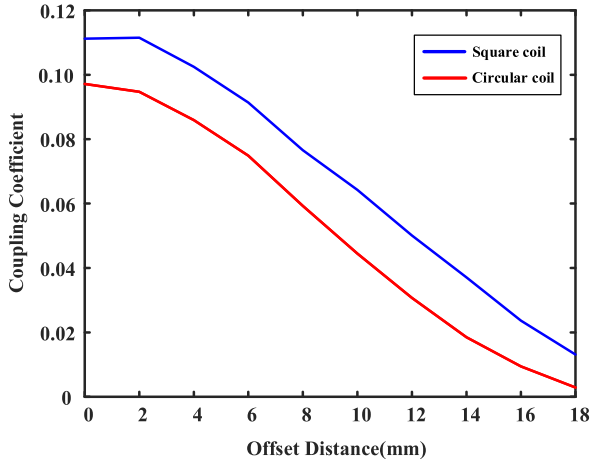

FIGURE 6. Comparison of the resistance to static offset.

The coupling degree of the coupling coils has a great influence on the transmission efficiency of the system, so its parameters design is very important [25], [26], [27], [28]. According to the analysis in the third section, the mutual inductance is correlated with turns and the distance. In addition, it should be noted that both the relative position of the transmitting and receiving coils, as well as the coupling degree of the rail-type coupler, change with variations in the rotation angle θ of the rotor. Hence, the rotation angle θ should also be considered during the optimization design process.

Next, the coupler is optimized through the finite element method to achieve optimal coupling performance. After the external circuit is constructed, the MAXWELL simulation model of the rail-type rotary coupler is imported. When the rotation angle θ is set to 0°, the relationship between mutual inductance, efficiency, and the number of coil turns can be obtained. As shown in Fig. 7, the mutual inductance and the coupling efficiency first increase and then decrease with an increase in the number of turns. The growth rate of efficiency becomes very slow after 10 turns. Thus, the number of turns for both the transmitting coils and the receiving coils is chosen to be 10.

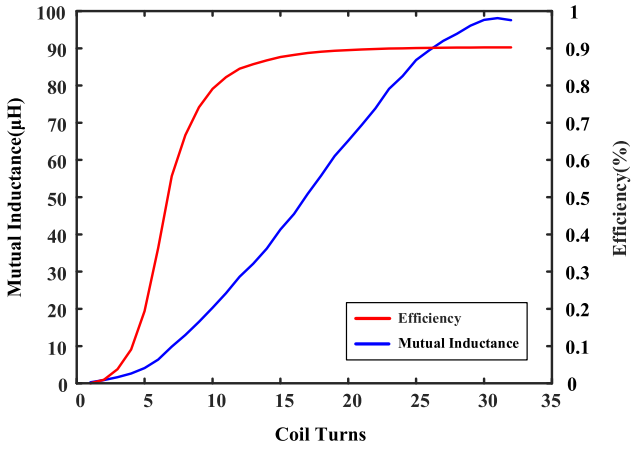

FIGURE 7. Mutual inductance and coupling coefficient with turns changing.

When the rotation angle θ is set to 0°, the relationship between mutual inductance, efficiency, and the distance separating the transmitting and receiving coils can be obtained. As shown in Fig. 8, the mutual inductance decreases with an increase in coils distance, and the coupling efficiency decreases rapidly after 40mm with an increase in distance. Therefore, in this paper, a distance of 2 cm is chosen between the transmitting coils and the receiving coils, which can prevent collisions caused by shaft vibrations and enhance system stability.

Finally, the fluctuation of I_{DC}, U_{out} and I_{out} of the RF-R-WPT system with rotation angle changing are obtained,

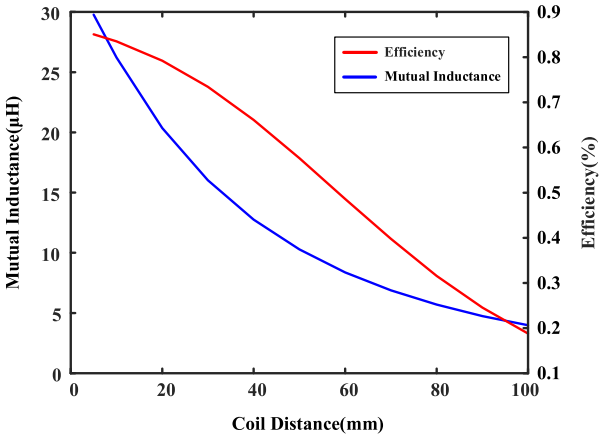

FIGURE 8. Mutual inductance and coupling coefficient with distance changing.

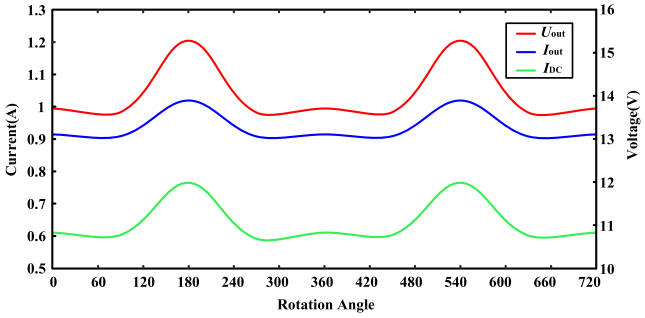

FIGURE 9. I_{DC}, U_{out}, I_{out} with rotation angle changing.

respectively, as shown in Fig.9. Furthermore, the mutual inductance, efficiency of the rail-type coupler with the rotation angle changing are shown in Fig. 10. It can be observed that when the rotor completes one full rotation (with θ ranging from 0° to 360°), the mutual inductance of the coupler experiences a certain decrease within the range of 90° to 270°, reaching a minimum value at 180°, and the mutual inductance changes once in one rotation cycle.

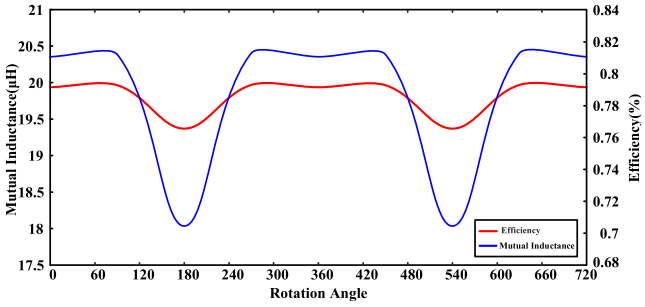

FIGURE 10. Mutual inductance and coupling coefficient with rotation angle changing.

Taking into comprehensive consideration, the final coils simulation parameters of the rail-type rotary coupler in this paper are shown in Table 1. The arcuate coupling coils, when flattened, takes the shape of a rectangle with straight side

TABLE 1. Parameters of coils.

Types	Parameters	Values
Transmitting coils	l_1(mm)	1800
	w_1(mm)	130
	d_1(mm)	2
	r_1(mm)	1
	R_1(mm)	286
	N_1	10
Receiving coils	l_2(mm)	400
	w_2(mm)	130
	d_2(mm)	2
	r_2(mm)	1
	R_2(mm)	266
	N_2	10

lengths of l_1 and l_2, and straight side widths of w_1 and w_2. d_1 and d_2 are the turn spacings of the transmitting coils and receiving coils, respectively. r_1 and r_2 are the Litz wire diameters of the transmitting coils and receiving coils, respectively. R_1 and R_2 are the circular radii of the cylinders formed by the transmitting coils and receiving coils, respectively. N_1 and N_2 are the turns of the transmitting coils and receiving coils, respectively.

To reduce the skin effect and proximity effect of the coil, the coil is made of the Litz wire in this paper. The copper core of the Litz wire used consists of 600 copper wires with a circular cross-section. Notably, the Litz wire is characterized by its excellent heat resistance, capable of withstanding temperatures up to 155°C. In addition, to enhance the mutual inductance and coupling coefficient of the coupling coils and reduce magnetic leakage, Mn-Zn ferrites (PC40) are incorporated for magnetic shielding on the coils in this system. The iron core is evenly distributed along the circumference of the coils, significantly reducing both its consumption and weight.

V. EXPERIMENT AND ANALYSIS

To validate the theory proposed in this paper, an experimental platform for RTR-WPT system is constructed, as shown in Fig. 11. The relevant experiment parameters are given in Table 2, and the rotational coupler is designed according to the preceding simulation results in Section IV.

The system is powered by a DC power supply with a 24V input voltage. A 100 kHz PWM control signal is provided by the STM32 microcontroller. The system employs an S-S compensation network, and metal polypropylene film capacitors (CBB) are used as compensation capacitors. The half-bridge inverter circuit is mainly composed of two MOSFETs (C2M0080120) and an IR2104s driver chip. The full bridge rectifier is mainly composed of four diodes (DSEI30-06A), and the system is loaded with a 15Ω resistance.

The experimental testing is conducted on the RTR-WPT system platform under static conditions, in which the rotor

TABLE 2. Experiment parameters.

Parameters	Values
f_0(kHz)	100
U_{DC}(V)	24
R_L(Ω)	15
R_T(Ω)	0.18
R_R(Ω)	0.48
L_T(μH)	43.5
L_R(μH)	188.2
C_T(nF)	58.2
C_R(nF)	13.4

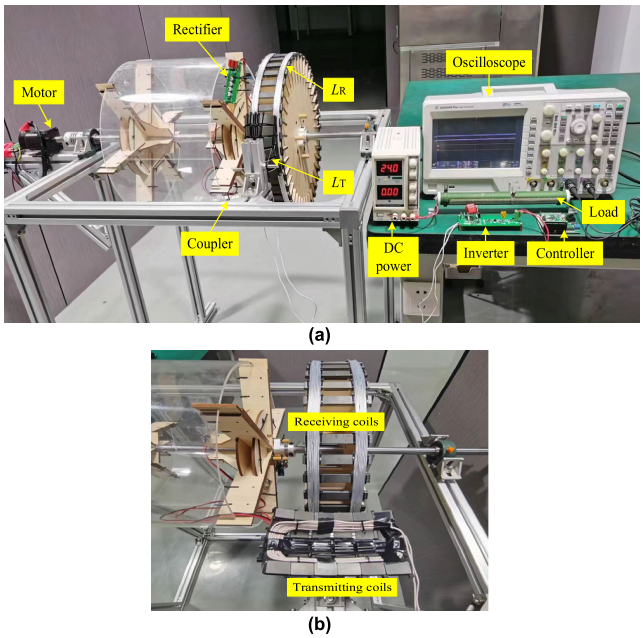

FIGURE 11. RTR-WPT system experimental platform. (a) Rotating experimental. (b) Radial flux coupler.

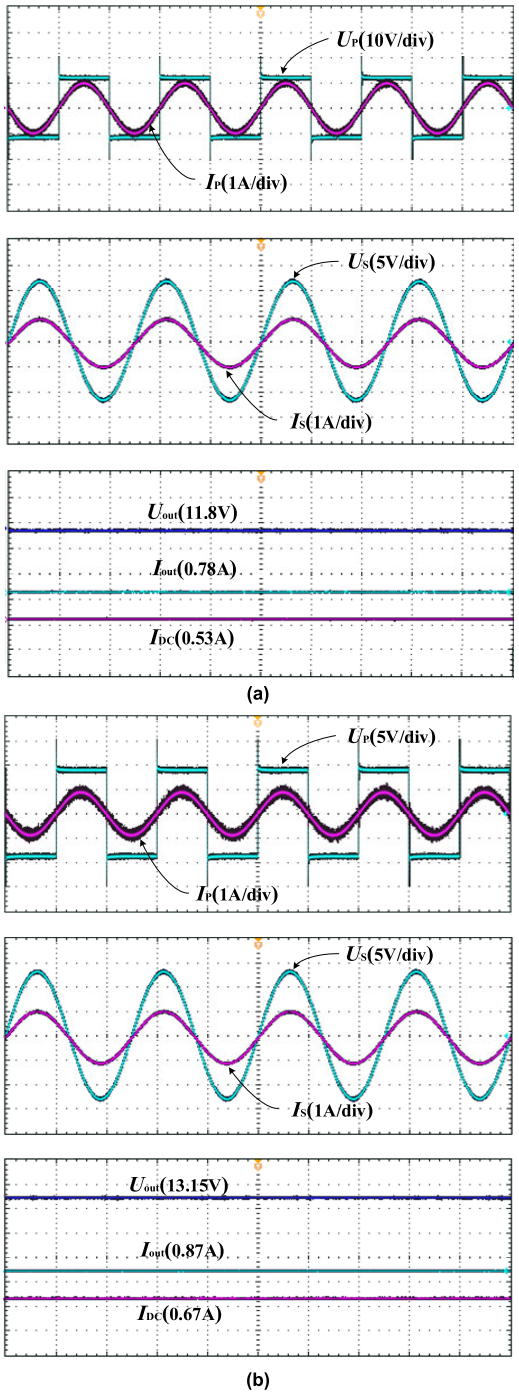

FIGURE 12. Experimental waveforms at different angles. (a) 0°. (b) 180°.

does not rotate. When the rotation angle θ are 0° and 180°, respectively, the experimental waveforms of U_P, I_P, U_S, I_S, I_{DC}, I_{out}, U_{out} are obtained, as shown in Fig. 12. It can be observed that the transmitting and receiving sides have consistent frequencies, and the voltage and current phases of the primary and secondary are the same. Thus, the system has achieved a unified resonant state.

Through experiments, system efficiency testing and loss analysis can be conducted. At $\theta = 0°$, the transmission efficiency is about 73%. The DC input power is 12.72W, the primary side input power is 12W, the secondary side output power is 10.856W, and the DC output power is 9.28W. As a result, the inverter sustains a loss of 0.72W, the magnetically coupled resonance section loss is 1.144W, and the rectifier bridge incurs a loss of 1.576W. Within the magnetically coupled resonance part loss, the primary components are coil loss, magnetic core loss, and resonant capacitor loss. Based on the equivalent resistance of the coil and capacitor, the coil loss can be determined to be 0.58W and the capacitor loss to be 0.15W. Consequently, it can be calculated that the magnetic core sustains a loss of 0.41W. At $\theta = 180°$, the transmission efficiency is about 71.7%. The DC input power is 16W, the primary side input power is 15.068W, the secondary side output power is 13.458W, and the DC output power is 11.44W. Therefore, the inverter sustains a loss of

0.93W, the magnetically coupled resonance section loss is 1.61W, and the rectifier bridge experiences a loss of 2.018W. Similarly, it can be deduced that the coil loss is 0.78W, the capacitor loss is 0.25W, and the magnetic core loss is 0.58W. From the calculation results, the proportion of rectifier loss is the largest. Among the losses of the magnetic coupler, coil loss accounts for the largest proportion, and the resonance capacitor loss accounts for the lowest proportion.

In addition, the fluctuation patterns of output power, efficiency, I_{DC}, U_{out}, and I_{out} of the RF-R-WPT system with varying rotation angles are obtained through measurements, as shown in Fig. 13 and Fig. 14. It can be seen that the measurement results are consistent with the previous simulations.

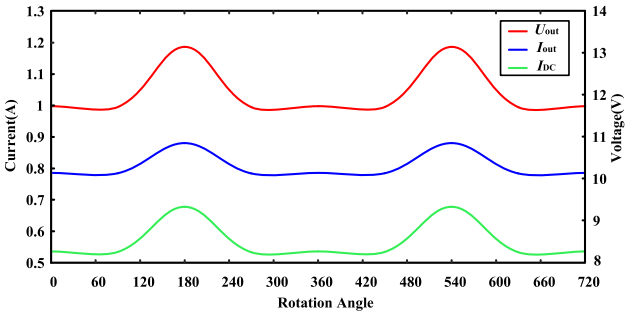

FIGURE 13. I_{DC}, U_{out}, I_{out} with rotation angle changing.

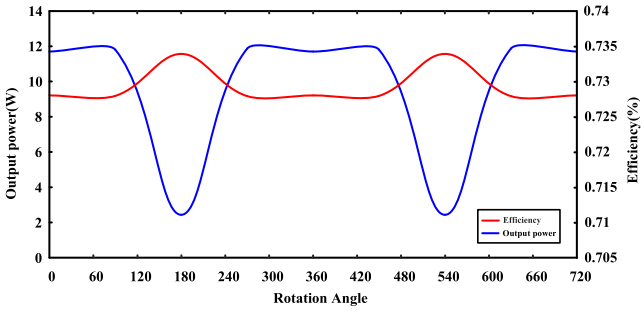

FIGURE 14. Output- power and coefficient with rotation angle changing.

The above experiments on transmission characteristics are performed under static conditions, to obtain the dynamic performance of the RTR-WPT system proposed in this paper, a rotation experiment is conducted. When the rotation rate are 150 r/min and 300 r/min, respectively, the experimental waveforms of I_{DC}, I_{out}, U_{out} are obtained, as shown in Fig. 15. It can be observed that the variation trends of I_{DC}, U_{out}, I_{out} under rotating conditions are consistent with the simulation results. The output power and efficiency are not influenced by rotate speed at this level, which is consistent with the previous analysis. Under the conditions of a 24V DC input voltage and maintaining a constant rotational speed, the average output power of the RTR-WPT system is about 10.33W, the average transmission efficiency is about 72.1%.

In summary, the input and output characteristics of the RTR-WPT system collected in the above experiment are in

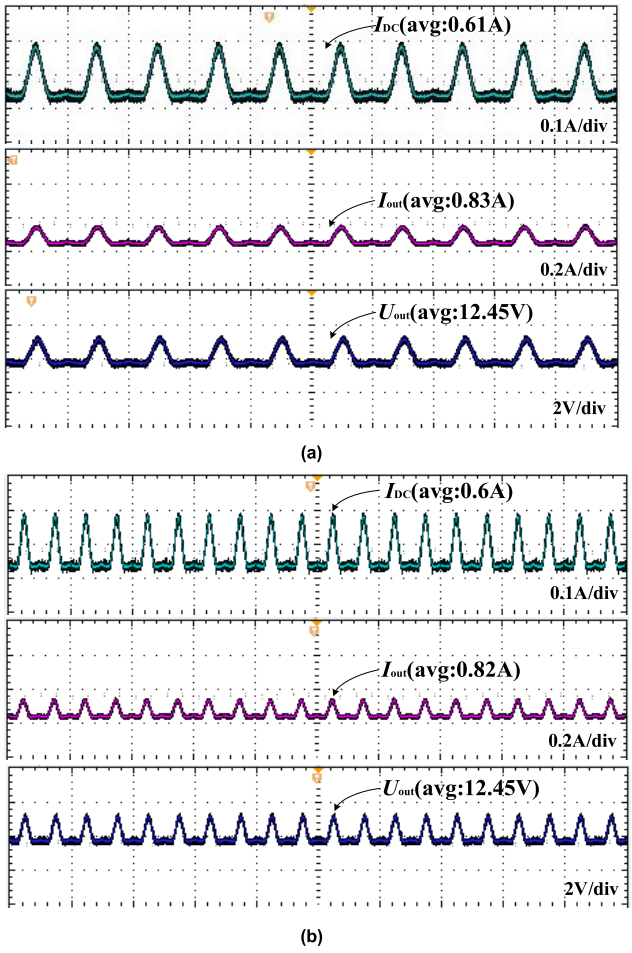

FIGURE 15. Experimental waveforms at different speeds. (a) 150r/min. (b) 300r/min.

accord with the previous analysis and meet the expected effects, thus validating the proposed theory and scheme.

The designed system is compared with the recent R-WPT systems in this paper, and the results are shown in Table 3. In comparison to [17] and [18], although our system has certain limitations in terms of efficiency and power level, it boasts a longer transmission distance and employs a coupling structure with distinct advantages. This structure does not require the high assembly precision demanded by cylindrical coupling methods, thus preventing potential component interference caused by improper installation. As a result, it enhances the system's reliability and makes it more suitable for high-speed applications. Additionally, the installation and disassembly processes are greatly facilitated. Furthermore, the coupling coil adopts a planar coil design, which compared to solenoidal coils, offers simpler winding, smaller size, lighter weight, and lower production costs, making it ideal for large-scale production and application. Compared to the decentralized parallel coils adopted in [19], the coupling coil proposed demonstrates higher stability under rotating conditions in this paper. Compared to [20], the proposed system exhibits better transmission performance.

TABLE 3. Comparison of different R-WPT systems.

Reference	Coupler	Power(W)	Efficiency(%)	Distance(mm)
[17]	Cylindrical nested coils	3000	92.7	10
[18]	Mixed axial and radial coupler	163.59	80	--
[19]	Multiple scattered parallel coils	1.75	75	3
[20]	U-shaped magnetic core coupler	1.72	51.19	15
This paper	Rail-type coupler	10.33	72.1	20

In summary, the described system exhibits good performance characterized by stable output, safety and reliability, high installation flexibility, and relatively long transmission distance in this paper.

VI. CONCLUSION

To address the current problems in rotary wireless power supply systems, a new RTR-WPT system is proposed in this paper. The working principle, compensation topology, and circuit model of the system are analyzed in this article. A rail-type rotary coupler is designed, and corresponding parameters design methods are provided. By optimizing the magnetic core structure, energy losses of the system are reduced. An experimental platform for the RTR-WPT system is constructed and tested. The experimental results align well with the simulation results, verifying the feasibility of the proposed design in this paper. Based on the results, it can be concluded that the new rail-type coupler is reliable and easy to install, and its coupling degree varies periodically with the rotation angle. The RTR-WPT system realizes a stable power output of 10.33W with a transmission efficiency of approximately 72.1% at the constant rotational speed, and the power and efficiency are not affected by rotation rate. The future work will focus on further improving system stability, integration, and transmission efficiency.

REFERENCES

[1] W. Liu, K. T. Chau, X. Tian, H. Wang, and Z. Hua, "Smart wireless power transfer—Opportunities and challenges," *Renew. Sustain. Energy Rev.*, vol. 180, Jul. 2023, Art. no. 113298.
[2] S. Luo, A. Qiao, and Q. Tang, "A magnetic coupled rotary composite force sensor," *IEEE Sensors J.*, vol. 20, no. 2, pp. 745–751, Jan. 2020.
[3] Y. Zhou, Y. Luo, S. Liu, and D. Li, "An efficient and stable embedded multi-U-shaped column rotary transformer," *IEEE Trans. Power Electron.*, vol. 38, no. 5, pp. 6734–6743, May 2023.
[4] Y. Zhang, J. Yang, D. Jiang, D. Li, and R. Qu, "Design, manufacture, and test of a rotary transformer for contactless power transfer system," *IEEE Trans. Magn.*, vol. 58, no. 2, pp. 1–6, Feb. 2022.
[5] W. Zhou, Z. Zhu, R. Mai, and Z. He, "Design and analysis of decoupled tetra-polar ring-coils for wireless power transfer in rotary mechanism applications," *IET Electr. Power Appl.*, vol. 14, no. 10, pp. 1766–1773, Oct. 2020.
[6] G. Rizzoli, M. Mengoni, A. Tani, G. Serra, L. Zarri, and D. Casadei, "Wireless power transfer using a five-phase wound-rotor induction machine for speed-controlled rotary platforms," *IEEE Trans. Ind. Electron.*, vol. 67, no. 8, pp. 6237–6247, Aug. 2020.
[7] Z. Wei, B. Zhang, S. Lin, and C. Wang, "A self-oscillation WPT system with high misalignment tolerance," *IEEE Trans. Power Electron.*, vol. 39, no. 1, pp. 1870–1887, Jan. 2024.
[8] R. Manko, M. Vukotić, D. Makuc, D. Vončina, D. Miljavec, and S. Čorović, "Modelling of the electrically excited synchronous machine with the rotary transformer design influence," *Energies*, vol. 15, no. 8, p. 2832, Apr. 2022.
[9] A. Mahesh, B. Chokkalingam, and L. Mihet-Popa, "Inductive wireless power transfer charging for electric vehicles—A review," *IEEE Access*, vol. 9, pp. 137667–137713, 2021.
[10] S. Li, X. Yu, Y. Yuan, S. Lu, and T. Li, "A novel high-voltage power supply with MHz WPT techniques: Achieving high-efficiency, high-isolation, and high-power-density," *IEEE Trans. Power Electron.*, vol. 38, no. 12, pp. 14794–14805, Dec. 2023.
[11] K. Chen and Z. Zhang, "In-flight wireless charging: A promising application-oriented charging technique for drones," *IEEE Ind. Electron. Mag.*, vol. 18, no. 1, pp. 6–16, Mar. 2024.
[12] Y. Li, W. Sun, J. Liu, Y. Liu, X. Yang, Y. Li, J. Hu, and Z. He, "A new magnetic coupler with high rotational misalignment tolerance for unmanned aerial vehicles wireless charging," *IEEE Trans. Power Electron.*, vol. 37, no. 11, pp. 12986–12991, Nov. 2022.
[13] Y. Zeng, C. Lu, R. Liu, X. He, C. Rong, and M. Liu, "Wireless power and data transfer system using multidirectional magnetic coupler for swarm AUVs," *IEEE Trans. Power Electron.*, vol. 38, no. 2, pp. 1440–1444, Feb. 2023.
[14] T. Campi, S. Cruciani, F. Maradei, A. Montalto, F. Musumeci, and M. Feliziani, "Centralized high power supply system for implanted medical devices using wireless power transfer technology," *IEEE Trans. Med. Robot. Bionics*, vol. 3, no. 4, pp. 992–1001, Nov. 2021.
[15] J. Gao, J. Zhou, C. Yuan, Z. Zhang, C. Gao, G. Yan, R. Li, and L. Zhang, "Stable wireless power transmission for a capsule robot with randomly changing attitude," *IEEE Trans. Power Electron.*, vol. 38, no. 2, pp. 2782–2796, Feb. 2023.
[16] C. Cai, J. Wang, L. Wang, Z. Yuan, N. Tang, X. Han, and S. Wang, "Improved coplanar couplers based WPT systems for adaptive energy harvesting on power towers," *IEEE Trans. Electromagn. Compat.*, vol. 63, no. 3, pp. 922–934, Jun. 2021.
[17] K. Song, B. Ma, G. Yang, J. Jiang, R. Wei, H. Zhang, and C. Zhu, "A rotation-lightweight wireless power transfer system for solar wing driving," *IEEE Trans. Power Electron.*, vol. 34, no. 9, pp. 8816–8830, Sep. 2019.
[18] L. Wang, J. Li, G. Luo, Q. Si, Z. Guo, Y. Peng, and I. Robertson, "A mixed flux coupler and dual-path parallel compensation based rotating wireless power transfer system integrated with rotational speed monitoring function," *IEEE Trans. Power Electron.*, vol. 39, no. 6, pp. 7736–7751, Jun. 2024.
[19] Y. C. Lee and V. A. Hoang, "Battery-free and real-time wireless sensor system on marine propulsion shaft using a wireless power transfer module," *Sensors*, vol. 23, no. 2, p. 558, Jan. 2023.
[20] J. Jinliang and Y. Xiaoqiang, "Research on characteristics of wireless power transfer system based on U-Type coupling mechanism," *J. Electr. Comput. Eng.*, vol. 2021, pp. 1–9, Feb. 2021.
[21] R. Yue, C. Wang, H. Li, and Y. Liu, "Constant-voltage and constant-current output using P-CLCL compensation circuit for single-switch inductive power transfer," *IEEE Trans. Power Electron.*, vol. 36, no. 5, pp. 5181–5190, May 2021.
[22] A. Vulfovich and A. Kuperman, "Design space of sub-resonant frequency-controlled series–series–compensated inductive wireless power transfer links operating with constant output current under frequency constraints," *IEEE J. Emerg. Sel. Topics Power Electron.*, vol. 10, no. 5, pp. 5414–5422, Oct. 2022.

[23] Z. Dai and J. Wang, "A dual-frequency WPT based on multilayer self-decoupled compact coil and dual CLCL hybrid compensation topology," *IEEE Trans. Power Electron.*, vol. 37, no. 11, pp. 13955–13965, Nov. 2022.
[24] X. Tang, Z. Chen, S. Zheng, H. Chen, X. Zhao, and Y. Kong, "Design of compensation network and parameter optimization for rotary ultrasonic machining under varying loads," *IEEE Trans. Power Electron.*, vol. 38, no. 11, pp. 14747–14760, Nov. 2023.
[25] Z. Dai, X. Zhang, T. Liu, C. Pei, T. Chen, R. Dou, and J. Wang, "Magnetic coupling mechanism with omnidirectional magnetic shielding for wireless power transfer," *IEEE Trans. Electromagn. Compat.*, vol. 65, no. 5, pp. 1565–1574, Oct. 2023.
[26] Y. Zhang, W. Pan, H. Wang, Z. Shen, Y. Wu, J. Dong, and X. Mao, "Misalignment-tolerant dual-transmitter electric vehicle wireless charging system with reconfigurable topologies," *IEEE Trans. Power Electron.*, vol. 37, no. 8, pp. 8816–8819, Aug. 2022.
[27] Y. Zhang, X. Wu, Y. Lei, J. Cao, and W.-H. Liao, "Self-powered wireless condition monitoring for rotating machinery," *IEEE Internet Things J.*, vol. 11, no. 2, pp. 3095–3107, Jan. 2024.
[28] Y. Huang, C. Liu, Y. Xiao, and S. Liu, "Separate power allocation and control method based on multiple power channels for wireless power transfer," *IEEE Trans. Power Electron.*, vol. 35, no. 9, pp. 9046–9056, Sep. 2020.

KUN XIA was born in China, in 1980. He received the B.Eng. degree in industrial automation and the Ph.D. degree in power electronics and power drives from Hefei University of Technology (HFUT), Hefei, China, in 2002 and 2007, respectively.

From 2007 to 2011, he was a Lecturer with the University of Shanghai for Science and Technology (USST), Shanghai, China. From 2011 to 2019, he was an Associate Professor and the Department Head of the Department of Electrical Engineering, USST. From 2015 to 2016, he was a Visiting Scholar with the Department of Electrical and Computer Engineering, National University of Singapore, Singapore. From 2020 to 2022, he was a Professor and the Vice President of the College of Innovation and Entrepreneurship, USST. Since 2022, he has been a Professor and the Vice President of the College of Mechanical Engineering, USST. He has been in charge of more than 50 research projects from the government and companies and published more than 80 articles. His research interests include motor and motor control and new energy application. He won the Third Prize of the Scientific and Technological Progress Award of Zhejiang Province, in 2017, and Shanghai, in 2020.

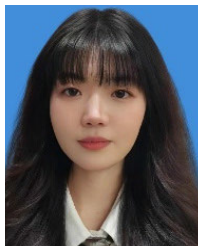

BENJING ZHU was born in China, in 2000. She received the B.Eng. degree from the Department of Electrical Engineering, Qingdao University of Technology, Qingdao, China, in 2021. She is currently pursuing the M.Eng. degree with the Department of Electrical Engineering, University of Shanghai for Science and Technology. Her current research interests include wireless power transmission and photovoltaic power generation.

YANG LOU was born in China, in 1999. He received the B.Eng. degree from the Department of Electrical Engineering and Its Automation, University of Shanghai for Science and Technology, Shanghai, China, in 2021. He is currently pursuing the M.Eng. degree with the Department of Electrical Engineering, University of Shanghai for Science and Technology. His current research interests include sensor measurement systems and embedded chips.

DAMING HUANG was born in China, in 1996. He received the B.Eng. degree from the Department of Electrical Engineering and Its Automation, Shanghai University of Electric Power, Shanghai, China, in 2019. He is currently pursuing the M.Eng. degree with the Department of Electrical Engineering, University of Shanghai for Science and Technology. His current research interests include dc/dc converter and wireless power transmission.